철 함유 모더나이트 분자체의 수열합성 및 특성연구

고용식*, 장현태[1], 안화승[2]
신성대학 신소재화학과, [1]한서대학교 화학공학과, [2]인하대학교 화학공학과
(ysko@shinsung.ac.kr*)

Hydrothermal Synthesis and Characterization of Iron-containing Mordenite

Yong Sig Ko*, Hyun Tae Jang[1], Wha Seung Ahn[2]
Department of Advanced Material Chemistry, Shinsung College,
[1]Department of Chemical Engineering, Hanseo University,
[2]Department of Chemical Engineering, Inha University
(ysko@shinsung.ac.kr*)

Introduction

Isomorphous substitution of Fe^{3+} into the framework of zeolites induces changes in acidity and modification in morphology, as well as pore expansion caused by introducing an Fe-O bond (1.84 Å) in the place of a Si-O bond (1.60 Å), which can affect the product selectivity [1]. Due to their interesting properties, zeolites isomorphously substituted with iron have been studied extensively [2-10]. Szostak and Thomas [2] were the first who deliberately synthesized a sodalite with significant quantities of Fe^{3+} in the framework. Over the years, a wide range of iron analogues such as MFI [3], MEL [4], MOR [5], MTT [6], MTW [7], LTL [8], NU-1 [9], and TON [10] were reported, and various characterization techniques were employed to demonstrate the structural incorporated iron in these zeolites.

Synthetic mordenites are used extensively as catalysts and adsorbents. The replacement of Al^{3+} by Fe^{3+} ions in the mordenite framework may give rise to novel materials with interesting applications. Iron can be substituted into the tetrahedral framework sites of a molecular sieve structure during synthesis [2,11,12]; however, the amount of Fe^{3+} incorporated and the purity of the resulting zeolites depend on the conditions of synthesis [11]. Though synthesis methods of iron-substituted mordenites have been reported, further investigation concerning the synthesis of iron-substituted mordenites with extensive characterization and catalytic evaluation would contribute towards a better understanding of the system. In this work, we present the details of synthesis and characterization studies involving XRD, SEM, IR, ESR, UV-VIS DRS, and XAS for the zeolites having the MOR structure with associated iron species. Catalytic runs for toluene alkylation are also applied as a probe reaction to evaluate the property change.

Experimental

1. Synthesis

The reagents used in preparing the substrate were fumed silica (Cab-O-Sil, 97 % SiO_2), sodium hydroxide (Junsei Co., 95 %), sodium aluminate (Junsei Co., 32.6 % Na_2O, 35.7 % Al_2O_3), nanohydrate ferric nitrate (Shinyo Co., 98 %), and deionized water. The synthesis of Al- and Fe-substituted mordenite samples was conducted from substrates having the following compositions : $7\ Na_2O - x\ Fe_2O_3 - (1 - x)\ Al_2O_3 - 25\ SiO_2 - 700\ H_2O$, where x = 0, 0.15 and 0.30.

In a typical synthesis experiment, the reaction mixture was prepared by dissolving a desirable amount of ferric nitrate in deionized water to have solution A. Solution B was prepared by dissolving sodium hydroxide and sodium aluminate in deionized water. The required amount of fumed silica was added slowly to solution B with stirring until it was homogeneous. To this gel mixture solution A was slowly added with vigorous stirring until the homogeneous gel was obtained. The pH of gel mixture was adjusted by the addition of dilute sulfuric acid aqueous solution to the desirable value (pH≒10.5). The resulting pale yellow gel formed was further stirred for 1 h

intensively. The reaction mixture was transferred to a 100 ml teflon-lined stainless steel autoclave and maintained in an air oven at 443 K under unstirred conditions. Autoclaves were removed at different time intervals from the oven and were quenched immediately in cold water for phase identification. After the solid products were suction-filtrated, excess alkali was washed out with deionized water and the products were dried in an air oven at 393 K for 12 h.

2. Characterization

X-ray diffraction patterns of the different crystalline samples were determined by Philips, PW-1700 diffractometer using Ni-filtered monochromatic CuK α radiation, 40 kV, 25 mA with a scanning rate of 6° min^{-1} (2Θ). The crystallite size and morphology of the crystalline phase were examined using a scanning electron microscope (Hitachi, X-650) after coating with a Au-Pd evaporated film. Framework IR spectra of the samples were recorded in air at room temperature on a Perkin Elmer 221 spectrometer. Electron spin resonance spectra were measured with a Bruker E-2000 spectrometer in the temperature range of l00 K～300 K. Diffuse reflectance UV-vis spectra were recorded with a Varian CARY 3E spectrometer. The XAS spectra were measured above the Fe K-edge at beamline 10B, Photon Factory of National Laboratory for High Energy Physics in Tsukuba, Japan. EXAFS data were analyzed using UWXAFS2 program package.

Toluene alkylation with ethanol on the zeolites in their H^+-forms was carried out at atmospheric pressure at 623 K using a conventional fixed bed microreactor with 0.1 g catalyst pretreated in a hydrogen stream for 2 h at 773 K. The liquid mixture (2:1 mole ratio) of toluene/ethanol was fed to the evaporator using a syringe pump, and the hydrogen carrier then transported the reactant to the microreactor. The reaction products were analyzed by on-line GC using a 4.5 m column packed with 5 % Bentone-34 and 5 % diisodecyl phthalate on Uniport B.

Results and discussion

The crystallization kinetics for the Al- and Fe-substituted mordenite samples are shown in Figure 1. The percent crystallinity of the sample was determined by comparing the peak areas at $2\Theta = 9.79$, 13.55, 22.37, 25.76, 26.39 and 27.81 to those of the most crystalline zeolite sample obtained. All the curves exhibit a typical sigmoidal nature, characteristic of both the sequential processes of nucleation and crystal growth. The overall crystallization rates at constant gel composition and temperature decreased with increasing iron contents of the synthesis gel. The increase in iron content in the synthesis gel was found to cause a decrease in the rate of nucleation (longer induction period) and to extend the crystallization period needed to obtain fully crystalline sample.

IR spectrum of partially Fe-substituted mordenite showed a pattern similar to the one corresponding to normal Al-mordenite. In these spectra, the absorption bands originating from iron hydroxides and iron oxides were not observed. Upon introducing Fe in the zeolite framework, IR absorption bands shifted towards the lower frequency region compared with those of the iron free mordenite ; the bands at 1227 and 810 cm^{-1}, due to asymmetric and symmetric stretching vibrations of Si-O-T (T=Al), were shifted to 1200 and 788 cm^{-1} on isomorphous substitution of Al by Fe atoms in the lattice framework. The shift to lower frequency in the spectra is due to increases in the unit cell parameters caused by Fe^{-1} existing on tetrahedral sites, and similar results for other ferrisilicates have been reported earlier [13,14].

In zeolites, the closeness in mass between Si and Al does not give rise to distinct contributions from the $-(Si\text{-}O\text{-}Si)_n-$ and $-(Si\text{-}O\text{-}Al)_n-$ vibrations [15]. However, in the ferrisilicate, silicon and iron are sufficiently different in atomic weight to change the reduced mass of the harmonic oscillator when iron is substituted for silicon. This difference can be sufficient to produce separate bands [16]. Accordingly, in the partially Fe-substituted mordenite, a new Si-O-Fe bond vibration could be found near 668 cm^{-1}, which is absent in the IR spectrum of normal mordenite. Szostak and Thomas [2] have found that Si-O-Si symmetric stretching vibration appeared at 786 cm^{-1} and the Si-O-Fe symmetric stretching vibration occur at 679 cm^{-1} in the sodalite system. They also reported that the absorption originated from the vibration of Fe-O-Si is observed at 656 cm^{-1} in the spectra of ferrisilicate ZSM-5 [11].

Figure 2 shows ESR spectra of the as-synthesized partially Fe-substituted mordenite. The use of ESR spectroscopy as a technique for detecting the presence of framework Fe^{3+} has been discussed by several authors, although the detailed interpretation of the ESR spectra is still a matter of debate. The ESR spectra of the sample reveal two signals ; a sharp signal at g = 4.3 assignable to tetrahedral Fe(III) and a broad signal at g = 2.0 assignable to octahedrally coordinated Fe^{3+} in non-framework positions. The enhanced intensity of the g = 4.3 signal at lower temperature as well as its relative insensitivity to oxidation-reduction treatments suggests that it arises from Fe^{3+} ions in tetrahedral lattice positions rather than non-framework positions. Just about every work dealing with Fe-substitution in molecular sieves shows both g = 4.3 and g = 2.0 signals in the ESR spectra even when completely isomorphous substitution is clamed, and their relative size and their variation with the iron concentration also vary depending on the zeolite system. ESR is predominantly used to check the g = 4.3 signal in order to confirm the tetrahedral substitution.

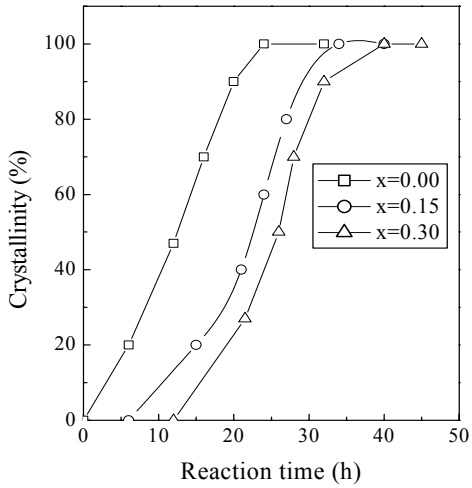

Figure 1. Crystallization curves for Al- and Fe-substitution mordenite samples.

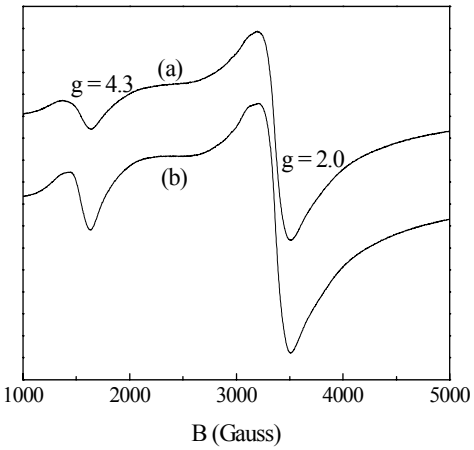

Figure 2. ESR spectra of Fe-substituted mordenite at (a) 297 K and (b) 100 K.

X-ray absorption spectroscopy (XAS) at the Fe K-edge was performed to collect information on the chemical state and the environment of Fe^{3+} in the partially Fe-substituted mordenite framework. Below the absorption edge, a pre-edge peak was found near 7112 eV. It corresponds to transitions from 1s to 3d-like levels. In an octahedral environment, this peak is weak due to the presence of an inversion center and two components are generally observed. In a tetrahedral environment, the pre-edge peak intensity is higher and only one single peak was found for Fe-containing glasses. The qualitative information deduced from the XANES has been complemented by the EXAFS study. According to the XAS, the Fe-O distance and Fe-O coordination number for Fe-substituted mordenite (x = 0.15) were 1.86 Å and 4.1, respectively. We have taken the data using a transmission mode in relatively short time, and its signal to noise ratio was sufficient enough to conduct the 1st shell calculations to estimate the Fe-O coordination number and its interatomic distance. Certainly, the Fe-O-Si(Al) coordination number and its distance would provide a more definite supporting evidence of the isomorphous Fe-substitution, but this type of calculation demands more efforts involving molecular modeling and it is necessary to take the data in a fluorescence mode which requires substantially longer synchrotron radiation beam time. The XAS results overall indicate that the majority of the iron was substituted into the mordenite framework.

Finally, the toluene alkylation reaction with ethanol at 623 K under atmospheric pressure was conducted as a probe reaction. The activity in terms of toluene conversion with Fe-substituted mordenite was lower compared with that of the normal Al-mordenite, as expected from the decreased

acid strength of the former [17]. In this case, the large reduction in conversion may also be a consequence of Fe^{3+} released from the zeolite structure blocking the uni-dimensional pores at high calcination/pretreatment temperature (773 K). Further investigations are in progress. For the Fe-substituted mordenite, the ethyltoluene selectivity in product distribution seems enhanced whereas the xylene selectivity was almost similar for both the samples. In this probe reaction study, however, the comparison of selectivity was not conducted at the same conversion level. It can be speculated that the modification of mordenite through isomorphous Fe^{3+} substitution resulted in substantial reduction of acid strength, and consequently the alkylation was promoted at the weakened acid sites. Disproportionation of toluene which requires strong acid sites cannot proceed due to weak acidity.

Conclusions

Isomorphous substitution of Fe^{3+} into mordenite was successfully carried out hydrothermally from the substrates in the composition range :

$7\ Na_2O - x\ Fe_2O_3 - (1 - x)\ Al_2O_3 - 25\ SiO_2 - 700\ H_2O$, where x = 0, 0.15 and 0.3.

The overall crystallization rates at constant gel composition and temperature decreased with increasing iron contents of the synthesis gel. The mid range IR spectra show a band shift to lower frequencies as the Fe^{3+} ions into the lattice incorporate, and a new Si-O-Fe bond vibration was located near 668 cm^{-1}. The ESR spectra show a signal at g = 4.3, which can be assigned to Fe^{3+} isomorphously substituted in the tetrahedral positions. EXAFS at the Fe K-edge revealed that the Fe^{3+} ions were present in the zeolite framework in a four-fold coordination with an average Fe-O distance of 1.86 Å. In the UV-vis spectra, the absorption at 375.7 nm was observed only for the Fe-substituted mordenite samples. A toluene alkylation probe reaction study indicated that lattice iron species in mordenite weakened the acid strength and the ethyltoluene selectivity was enhanced as a result.

Acknowledgement

This research was supported by a grant (code DD2-101) from Carbon Dioxide Reduction & Sequestration Research Center, one of the 21st Century Frontier Programs funded by the Ministry of Science and Technology of Korean government.

References

[1] M. Tielen, N. Geelen and P.A. Jacobs, *Acta. Phys. Chem.*, **31**, 1 (1985).
[2] R. Szostak and T.L. Thomas, *J. Chem. Soc., Chem. Commun.*, 113 (1986).
[3] A. Meagher, V. Nair, and R. Szostak, *Zeolites*, **8**, 3 (1988).
[4] J.S. Reddy, K.R. Reddy, R. Kumar, and P. Ratnasamy, *Zeolites*, **11**, 553 (1991).
[5] A.J. Chandwadkar, R.N. Bhat, and P. Ratnasamy, *Zeolites*, **11**, 42 (1991).
[6] R. Kumar and P. Ratnasamy, *J. Catal.*, **121**, 89 (1990).
[7] Zhao Yanan and Li Xi Hexuan, *Shiyou Xuebao, Shiyou Jiagong*, **6**, 33 (1990).
[8] Y.S. Ko and W.S. Ahn, *Microporous and Mesoporous Materials*, **9**, 131 (1997).
[9] G. Bellusi, R. Millini, A. Carati, G. Madinelli, and A. Gervasini, *Zeolites*, **10**, 642 (1990).
[10] R.B. Borade, A. Adnot, and S. Kaliagine, *Zeolites*, **11**, 710 (1991).
[11] R. Szostak and T.L. Thomas, *J. Catal.*, **100**, 555 (1986).
[12] R. Szostak, V. Nair, and T.L. Thomas, *J. Chem. Soc., Faraday Trans. 1.*, **83**, 487 (1987).
[13] P.N. Joshi, S.V. Awate, and V.P. Shiralkar, *J. Phys. Chem.*, **97**, 9749 (1993).
[14] R. Kumar, A. Thangaraj, R.N. Bhat, and P. Ratnasamy, *Zeolites*, **10**, 85 (1990).
[15] E.M. Flanigen, in J. Rabo (Ed.), *Zeolite Chemistry and Catalysis*, Am.Chem. Soc., p. 201, Washington DC (1971).
[16] F. Hazel, R.U. Schock, and M. Gordon, *J. Am. Chem. Soc.*, **71**, 2256 (1949).
[17] G. Calas and Petiau, *J. Solid State Commun.*, **48**, 625 (1983).